Structural And Optical Properties Of Plasma Polymerized Pyromucic Aldehyde Thin Films

Humayun Kabir[1], M. Mahbubur Rahman[1], Tanu Shree Roy[2], A.H. Bhuiyan[3]

[1]Department of Physics, Jahangirnagar University, Savar, Dhaka-1342, Bangladesh
[2] Department of Applied Science, Bangladesh University of Textiles, Tejgoan, Dhaka, Bangladesh
[3] Department of Physics, Bangladesh University of Engineering and Technology, Dhaka-1000

***Abstract*-- Plasma polymerized pyromucic aldehyde (PPPA) thin films have been deposited on to glass substrates by glow discharge technique. Scanning electron microscopy (SEM) graphs reveal that the surface morphology of PPPA thin films is uniform and flawless. FTIR analysis reveals that the chemical composition of PPPA films is different from that of the pyromucic aldehyde (PA). From the UV-vis spectra direct and indirect transition energy gaps were determined for as deposited PPPA thin films of different thicknesses.**

***Index Term*-- Plasma polymerized pyromucic aldehyde (PPPA) thin films, Scanning electron microscopy, FTIR spectroscopy, direct and indirect transition energy gap.**

1. INTRODUCTION

Plasma polymerization is a process of new material preparation and is not a kind of conventional polymerization. Polymerization conventionally refers to the molecular polymerization, that is, the chemical structure of a polymer can be derived from the chemical structure of the monomer. In contrast to such molecular processes, polymer formation in plasma has been recognized as an atomic (non-molecular) process [1]. The preparation processes like chemical vapor deposition, plasma chemical vapor deposition, ion-assisted vapor deposition, sputter coating of polymers, etc are all fall into category of non-molecular process. [2]. In plasma polymerization, a glow discharge is used to create active species such as radicals and ions from the monomer vapor so that polymer films are deposited through reactions between these active species present in gas phase and the surface of the sample.

The neutral species entering the reactor produce reactive fragments since energy is transferred by the electrons at a low-temperature, low pressure plasma environment and the substrate molecules are activated by exposure to the plasma environment and chemical bonds are formed among the reactive fragments [3].

Address for correspondence: Humayun Kabir, Assistant Professor, Department of Physics, Jahangirnagar University, Savar, Dhaka-1342, Bangladesh. E-mail: rumy140@yahoo.com, Mobile: 01747180136

The chemical structure of a plasma polymer is not exactly matches to that of the monomer, largely due to abstraction of hydrogen atoms [4]. Plasma polymer films have potential application in microelectronics, optoelectronics, biomedical, membrane separation, biosensors, coatings, insulating layers, etc. [5, 6]. Tengku Nadzlin Bin Tengku Ibrahim et al. [7] prepared organic films by plasma polymerization method using naphthalene and propane as starting monomers. The aromatic and aliphatic rings found in infrared transmission for all samples showed that the samples contained the monomer chemical structure. Xiong-Yan Zhao et al. [8] prepared poly(4-biphenylcarbonitrile) (PBPCN) thin films using plasma polymerization technique. They studied the effect of discharge power on the chemical structure and surface compositions of PBPCN thin films using Fourier transform infrared (FTIR), Ultraviolet-visible (UV-vis) absorption and X-ray photoelectron spectroscopies. UV-vis. spectra show that a larger π-conjugated system can be formed in the PPBPCN thin films at low plasma discharge of 30 W. The FTIR results suggest that the plasma polymerization of 4-biphenylcarbonitrile has proceeded mainly via the opening of π-bonds of the C ≡ N functional groups under low discharge power of 30 W. For PBPCN50 films deposited at 50 W, however, a quite different FTIR absorption was observed as compared with that of the PBPCN30 film. A high discharge power of 50 W brings about more severe molecular (aromatic ring) fragmentation and thus the conjugation length of PBPCN films decreases due to the formation of a non-conjugated polymer. I. –S. Bae et al. [9] deposited plasma polymerized organic thin films on Si and glass substrates by plasma enhanced chemical vapor deposition (PECVD) method using methylcyclohexane and ethylcyclohexane as organic precursors. The structural and optical properties of the polymerized thin films were investigated by FTIR and UV-vis spectroscopy respectively. It was observed that as the plasma power was increased, the main IR absorption peak intensity of thin films was increased while the transmittance of the UV-vis spectra was decreased indicating high cross-linked density. The increase of absorption peak intensity with increasing the

RF power can be explained with either the increase of carbon contents or the scattered reflection caused by plasma bombardment. H. Akther and A. H. Bhuiyan [10] determined the direct (E_{qd}) and indirect transition (E_{qi}) energy gaps of as deposited and heat treated plasma polymerized N,N, 3,5-tetramethylaniline (PPTMA) thin films by UV-visible spectroscopy . The values of E_{qd} and E_{qi} are determined to be 2.80 and 1.56 eV, respectively.

This paper represents the preparation of thin films of pyromucic aldehyde by plasma polymerization technique. The chemical structure of PPPA by FTIR spectroscopy, optical properties by UV-vis spectroscopy and surface morphological study by scanning electron microscopy (SEM) have been investigated. These studies have been performed on the PPPA thin film of different thicknesses.

2. EXPERIMENTAL DETAILS

2.1 The monomer and the substrates

Pyromucic aldehyde ($C_5H_4O_2$) (Fig.1, tech. grade 90%, Aldrich chemical company, USA) in liquid form was used as organic precursor. Glass slides (18 mm×18 mm×1mm) (Sail brand, China) were used as substrates in this work. Before thin film deposition the substrates were cleaned with acetone and distilled water in an ultrasonic bath. The cleaned glass slides were then dried.

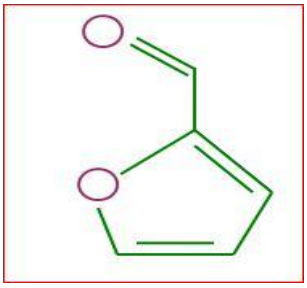

Fig. 1. Pyromucic aldehyde structure

2.2 Plasma polymerization

A capacitively coupled reactor was used for deposition of plasma polymerized PA (PPPA).The reactor consists of three parts, namely, vacuum system, gas inlet system and discharge system. The glow discharge system has two stainless steel parallel circular plates with a diameter of 0.09 m and thickness of 0.01 m placed 0.04 m apart. The substrates were positioned at the center on the lower electrode. A round bottom flask was used as the monomer container. Prior to the polymerization process the glow discharge chamber was evacuated by a rotary pump (Vacuubrand, Germany) down to a base pressure of about 1.33 Pa. Plasma was generated in the chamber with a step-up transformer by applying a potential of about 850 V between the electrodes at the line frequency 50 Hz. During the reaction, a vacuum gauge was used to measure the pressure inside the plasma chamber. Monomer vapor was injected into the reactor through a flow meter at a flow rate of about 20 cm^3/ min. During polymerization the power of the glow discharge was kept at about 40 W and deposition was made for 60 minutes. After the plasma was extinguished, the chamber was evacuated for 15 minutes and the films were taken out for characterization. The thickness of the plasma polymerized films deposited on glass substrates was measured by using a multiple-beam interferometric method [11].

2.3 Characterization techniques

2.3.1 Surface morphology

The surface morphology of the PPPA thin films have been investigated by SEM. Prior to SEM recording the film surface was coated with a thin layer of gold by sputtering (AGAR Auto Sputter Coater). SEM photographs of PPPA thin film surface were obtained by using a scanning electron microscope (S-3400N Hitachi, Japan).

2.3.2 Fourier transform infrared spectroscopy

The FTIR spectra of PPPA were recorded at room temperature by using a double beam IR spectrophotometer (SHIMADZU, FTIR-8900 spectrophotometer, JAPAN) in the wavenumber range of 400-4000 cm^{-1}. The FTIR spectrum of the monomer PA was obtained by putting the liquid monomer in a potassium bromide (KBr) measuring cell. PPPA powder was collected from the PPPA deposited substrates and then pellets of PPPA powder mixed with KBr were prepared for recording the FTIR spectra of various PPPA samples. FTIR spectra were recorded for as-deposited PPPA samples for different thicknesses. The FTIR spectra of the PA and the PPPA were recorded in transmittance (%) mode.

2.3.3 Ultraviolet-visible spectroscopy

The optical properties of the PPPA thin films deposited on to glass substrates having a dimension of 18mm×18mm×2mm were studied by UV-vis spectroscopic measurements. UV-vis absorption spectra were recorded using a dual beam UV-vis spectrophotometer (SHIMADZU UV-1601, JAPAN) in the wavelength range of 190-800 nm at room temperature. The absorption spectra were recorded both for PA and PPPA thin films as-deposited. Samples of thicknesses 125,175, 250, 350 and 400 nm were used for UV-vis spectroscopic studies. A blank glass slide was used as the reference during the optical absorption measurements.

3. RESULTS AND DISCUSSION

3.1 Scanning electron microscopy

Scanning electron micrographs of PPPA thin films were taken for magnification of 15k×, one of which is shown in Fig. 2.

From the micrographs it can easily be visualized that the surface of the plasma polymerized thin films is uniform, flawless, pinhole free and fracture free.

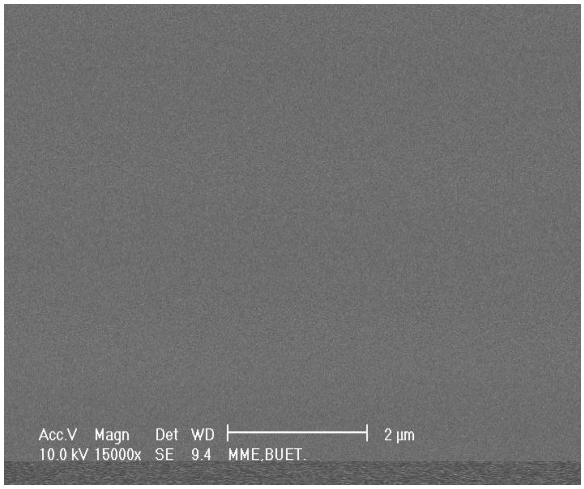

Fig. 2. SEM micrograph of the as-deposited PPPA thin film.

3.2 Fourier transform infrared spectroscopy (FTIR)

The FTIR spectra of PA and PPPA as-deposited are shown in Fig. 3 as curves P and Q respectively. These spectra reveal the structural changes due to plasma polymerization of the monomer PA. In the spectrum P of the monomer PA and spectrum Q of the PPPA a broad band at about 3133 and 3371 cm^{-1} (A), respectively are due to the presence of O-H stretching vibration for absorbed water. The characteristic absorption band in Q at 2925 cm^{-1} (B) may be assigned to aromatic C-H stretching vibration. The wider bands observed at 2850, 2811 (C) in the monomer spectrum may be due to aliphatic –O-CH_3 attached to Pyromucic aldehyde. The C≡C in Q at 2211 cm^{-1} (D) may be arisen due to plasma polymerization. The aliphatic conjugation C=C stretching vibration band at 1689 and 1674 cm^{-1} (E) is observed in monomer. The band at 1632 cm^{-1} (E) in PPPA is observed due to conjugation during polymerization.

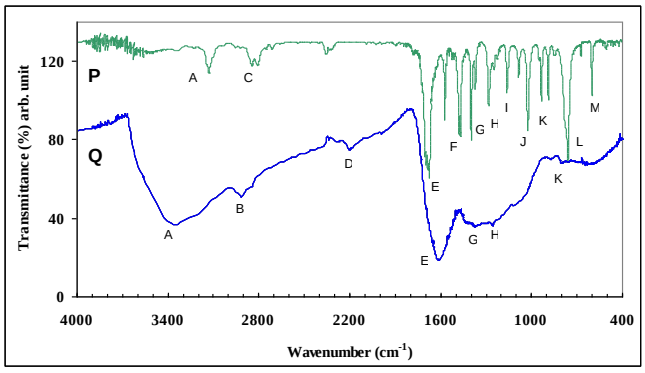

Fig. 3. The FTIR spectra for monomer PA (P) and PPPA as-deposited (Q)

The absorption bands at 1472 and 1464 cm^{-1} (F) correspond to the asymmetric C-H bending (E) and 1393 and 1367 cm^{-1} (G) correspond to the symmetric C-H bending vibrations. A band at around 1278 cm^{-1} (H) in P and at 1262 cm^{-1} (H) in Q is due to C-H twisting. The band at 1157 cm^{-1} (I) in only P represents a C-C skeletal vibration. In spectrum P, the bands at 1082 and 1020 cm^{-1} (J) correspond to the C=H in plane bending. The absorption bands at 930 and 883 cm^{-1} (K) in P may be arisen due to C-H rocking vibrations. The sharp absorption peaks at 755 cm^{-1} (L) is due to =C-H out-of-plane bending vibrations and the absorptions at 594 cm^{-1} indicate C=C out of plane bending. For comparison, the assignments to the different FTIR absorption bands of these two samples are presented in Table I.

TABLE I
Assignments of FTIR absorption bands for PA and PPPA.

Assignments	**Wavenumber (cm^{-1})**	
	PA (P)	PPPA (Q)
O-H stretching vibration (A)	3133	3371
Asym. C-H stretching vibration (B)	-------	2925
Aliphatic -O-CH_3 vibration (C)	2850, 2811	-------
C≡C stretching vibration(D)	-------	2211
C=C stretching vibration (E)	1689, 1674	1632
Asym.C-H bending (F)	1472,1464	-------
Symmetric C-H bending (G)	1393, 1367	1379
C-H twisting (H)	1278	1262
C-C skeletal vibration (I)	1157	-------
C=H plane bending (J)	1082,1020	-------
C-H rocking (K)	930, 883	-------
=C-H out of plane bending (L)	755	-------
C=C out-of-plane bending (M)	594	-------

3.3 Ultraviolet-visible spectroscopy

Amorphous films have a random network in contrast to the crystalline structure. In these materials no long range order is present. The disorder, associated with the deficiency of long range order in these materials, introduces a low density of localized electronic states in the band gap which influence the electronic properties of the material.

In Table I, it is seen that the chemical structure of as-deposited PPPA thin films contains C=C and C≡C conjugation instead of C-C skeletal structure. Therefore, it is observed from the above discussion that the structure of the PPPA thin films deposited by plasma polymerization process deviates to some extent from that of the PA structure (spectrum P). However these observations indicate that the aromatic ring structure is retained to a large extent in the PPPA thin films. It is seen from the FTIR spectra of the PPPA thin films that the intensity of the absorption bands decreased significantly compared to that of the monomer spectrum. This is an indication of monomer fragmentation during plasma polymerization.

The UV-Vis absorption spectra for PA and as-deposited PPPA thin films of different thicknesses have been recorded at room temperature as shown in Fig. 4. The absorbance increases with increasing thickness of the PPPA thin films and the absorption peak broadens as thickness increases. In all the spectra the intensity falls rapidly up to about 500 nm and then decrease slowly. The maximum peak wavelength value shifts to the higher wavelength compared to the peak wavelength value, 300 nm of the liquid monomer (inset of Fig.4). Absorption edge shifts to the higher wavelength of about 20 nm in comparison to that of the PA. It is known that increasing the length of the conjugated π-system generally moves the absorption maximum to longer wavelengths [12-13]. The red shift in PPPA thin films may be due to the presence of conjugation in the thin films. The absorption coefficient, α, was calculated from the absorption data for samples of different thickness using the relation [14] $\alpha = \frac{2.303A}{d}$, where $A = \log_{10}\left(\frac{I_0}{I}\right)$ is the absorbance, d is the path length of the absorbing species and α is the absorption co-efficient.

One of the most significant optical parameters, which is related to the electronic structure, is the optical band gap. The optical band gap E_{opt} can be calculated by Tauc relation, $\alpha h\nu = B(h\nu - E_{opt})^n$, where hν is the incident energy, n is the parameter connected with distribution of the density of states and B is the proportionality factor, called Tauc parameter [15].

The value of B is a measure of the steepness of band tail density of states (Urbach region). The index n equals 1/2 and 2 for allowed direct transition and indirect transition energy gaps respectively. Thus, the allowed direct and indirect energy gaps of insulators and/or dielectrics can be determined from the straight-line plots of $(\alpha h\nu)^2$ versus hν and $(\alpha h\nu)^{1/2}$ versus hν respectively.

Fig. 4 represents the absorption coefficient α as a function of photon energy, hν, for all the as–deposited PPPA. The graph indicates that the edges follow an exponential fall for values of α below about 20000 cm^{-1}, in the low energy region. Therefore, the curves can be characterized by two different slopes indicating the presence of direct and indirect transitions in the PPPA. The reason of these exponential falling edges is due to the lack of long-range order or due to the presence of defects in the thin films [16].

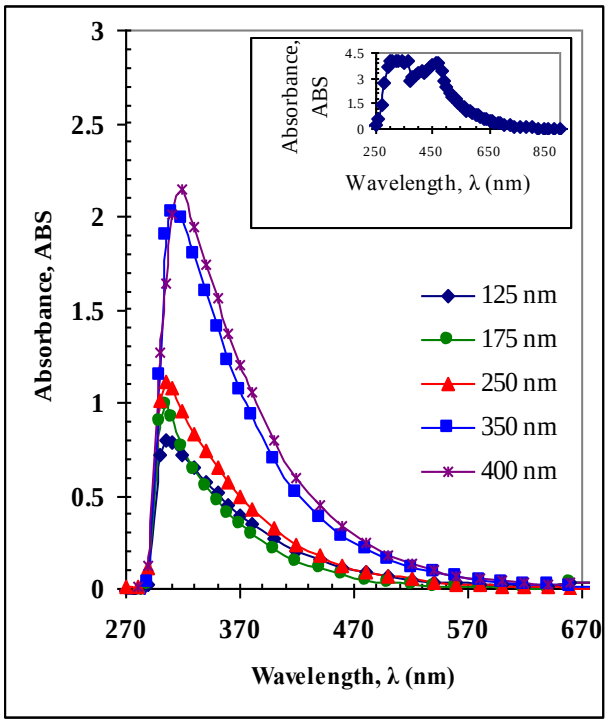

Fig. 4. Variation of absorbance, ABS, with wavelength, λ, for as-deposited PPPA thin films of different thicknesses [inset: monomer].

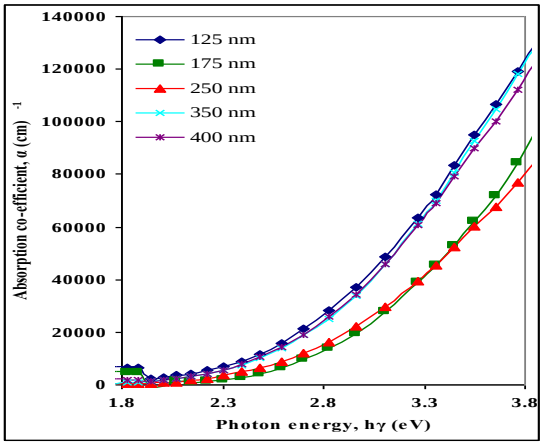

Fig. 5. Absorption coefficient, α as a function of photon energy, hγ, for as deposited PPPA thin films of different thickness.

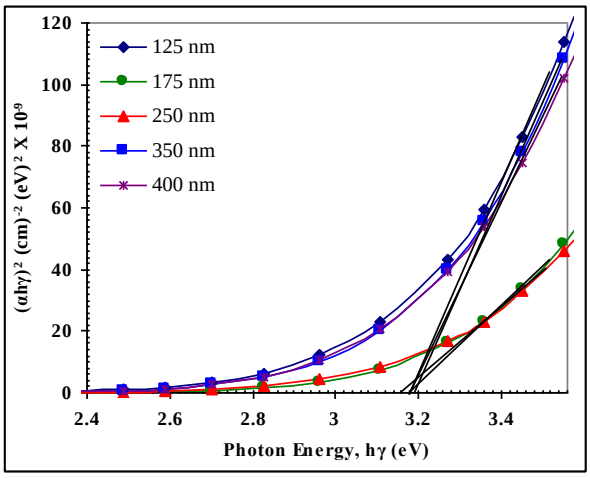

Fig. 6. $(\alpha h\nu)^2$ versus hν curves for as deposited PPPA thin films of different thicknesses.

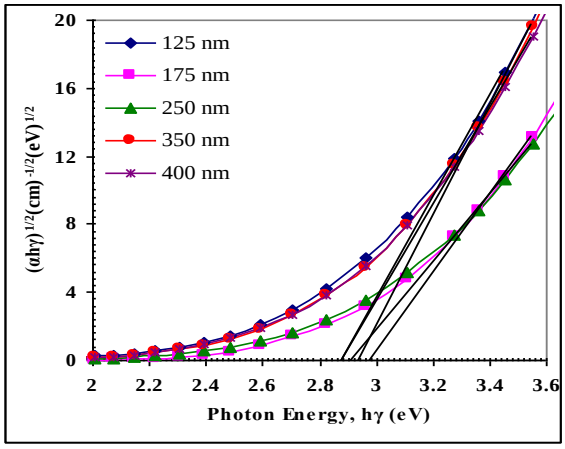

Fig. 7. $(\alpha h\nu)^{1/2}$ versus hν curves for as deposited PPPA thin films of different thicknesses.

The allowed direct transition energy gap (E_{qd}) can be calculated from the plots of $(\alpha h\nu)^2$ as a function of photon energy, hν, shown in Fig. 6 for as-deposited PPPA. E_{qd} is determined from the intercept of the extrapolation of the curve to zero α in the photon energy axis. In Fig. 7 $(\alpha h\nu)^{1/2}$ as a function of photon energy, hν, is plotted to obtain the allowed indirect transition energy gap (E_{qi}). The values of E_{qd} and E_{qi} obtained from the plots of Figs. 6 and 7 are documented in Table II. From Table II, it is seen that E_{qd} and E_{qi} do not follow any trend with thickness.

TABLE II
Values of allowed direct, $\mathbf{E_{qd}}$, indirect $\mathbf{E_{qi}}$ transition energy gaps for various PPPA thin films.

Sample	Film thickness d (nm)	E_{qd} (eV)	E_{qi} (eV)
As-deposited	125	3.18	2.88
	175	3.18	2.98
	250	3.16	2.92
	350	3.20	2.94
	400	3.18	2.88

4. CONCLUSIONS

As-deposited PPPA thin films are smooth, uniform and pinhole free. PPPA thin films may contain conjugation. The red shift in the maximum absorption wavelength for all the PPPA thin films was observed as compared with the monomer maximum absorption wavelength. The E_{qd} was found to be about 3.18-3.20 eV for as deposited PPPA. The E_{qi} was found to be about 2.88-2.98 eV for as deposited PPPA. The E_{qd} and E_{qi} do not follow any trend with thickness.

ACKNOWLEDGEMENTS

One of the authors (Humayun Kabir) is grateful to the authority of Bangladesh University of Engineering and Technology, Dhaka for financial assistance. He is thankful to the authority of Jahangirnagar University for permitting him to perform this research. He is also thankful to Mr. Nikhil Chandra Voumic, Officer, Wazed Miah Scientific Research Center for his help in taking FTIR spectra.

REFERENCES

[1] H. Yasuda, Plasma Polymerization, Academic Press, Inc. London (1985).
[2] Riccardo d'Agostino (Ed.), Plasma Deposition, Treatment, and Etching of Polymers, Academic Press, Inc., San Diego, 1990.
[3] Li-guang Wu, Chang-le Zhu, Moe Liu, Desalination **192**(2006)234.
[4] H. Biederman, Y. Osada, Polym. Phys., **95** (1990) 59.
[5] Hitoshi Muguruma, Tr. Anal. Chem., **26**(5) (2007) 433.
[6] N. F. Mott, Philos. Mag. **19** (1969) 835.
[7] Tengku Nadzlin Bin Tengku Ibrahim, Kunihiko Tanaka, Hisao Uchiki, Jpn. J. Appl. Phys. **47**(2008) 794.
[8] Xiang-Yan Zhao, Ming-Zhu Wang, Bing-Zhu Zhang, Lei Mao, Polym. Int. **56**(2007) 630.
[9] I.-S. Bae, C.-K. Jung, S.-J Cho, Y.-H. Song, J.-H. Boo, J. Alloys Comp. **449** (2008) 393.
[10] H. Akhter, A.H. Bhuiyan, Thin Solid Films **474**(2005)14.
[11] S. Tolansky, Multiple Beam Interferometry of Surfaces and Films, Clarendon Press, Oxford (1948).
[12] H. Xiao, Xiangyan Zhao, A. Uddin and C. B. Lee, Thin Solid Films **477** (2005) 81.
[13] J. H. Lambert, D. A. Lightner, H. F. Shurvell and R. G. Cooks, Introduction to Organic Spectroscopy, Macmillan, New York (1987).
[14] S.K.J. Al-Ani, A.A. Hiogazy, J. Matter. Sci. **26** (1991) 3670.
[15] J . Tauc, Optical Properties of Solids, F. Abeles Ed. North-Holland, Amsterdam (1972).
[16] E. A. Davis, N. F. Mott, Philos. Mag. **22** (1970) 903.